Propagating modes in planar and XY spin glasses

C. M. Grassl* and D. L. Huber
Department of Physics, University of Wisconsin—Madison, Madison, Wisconsin 53706
(Received 6 February 1984)

The low-lying harmonic magnons in two- and three-dimensional (2D and 3D) planar and XY spin glasses are investigated. Numerical calculations of the dynamic structure factor for $15\times15\times15$ (3D) and 30×30 (2D) arrays confirm the existence of the weakly damped, propagating modes reported earlier. In the case of the planar model, estimates of the spin-wave velocity inferred from the shift in the peak in the dynamic structure factor are in agreement with values obtained from a direct calculation of the stiffness by Grzonka and Moore. Numerical estimates of the densities of states are compared with the results obtained with the assumption of plane-wave eigenstates with velocities equal to the values inferred from the structure factor.

I. INTRODUCTION AND EQUATIONS OF MOTION

It is now believed that systems showing spin-glass characteristics have a highly degenerate manifold of ground states separated by barriers of varying heights.[1] This being the case, the low-lying excitations in spin glasses generally can be subdivided into intraconfigurational and interconfigurational modes. The latter involve transitions between different equilibrium configurations, each being a local minimum in the space of spin configurations. Intraconfiguration modes are excitations within a particular ground-state configuration. The interconfiguration modes are relaxational in character and are believed to be the mechanism responsible for the slow relaxation of the remanent magnetization. The intraconfigurational modes of vector spin glasses, i.e., Heisenberg and planar systems, are oscillatory being the spin-glass analog of magnons in translationally invariant systems.

An important question relating to intraconfigurational modes in the vector systems concerns the nature of the low-frequency excitations. According to hydrodynamic arguments,[2,3] there should exist weakly damped, long-wavelength, propagating magnon modes with a linear relationship between frequency and wave vector. Numerical as well as experimental studies have failed to establish the existence of such modes in Heisenberg spin glasses.[4,5] In contrast, numerical investigations have indicated that there are propagating modes in one model of a planar spin glass.[6–9]

In Refs. 6–9 the results of numerical studies of the linearized magnon modes associated with the planar Hamiltonian

$$\mathscr{H}=(1/2I)\sum_i (S_i^z)^2-\sum_{(i,j)} J_{ij}\vec{S}_i\cdot\vec{S}_j \tag{1.1}$$

are presented. The analysis was carried out in the limit $I^{-1}\gg J$, where the Villain transformation[10] can be used to write the equations of motion in the form

$$I\frac{d^2\phi_i}{dt^2}=-\sum_j A_{ij}\phi_j \ , \tag{1.2}$$

in which the dynamical matrix is given by

$$A_{ij}=\delta_{ij}S\sum_k J_{ik}\cos(\theta_i^0-\theta_k^0) -(1-\delta_{ij})SJ_{ij}\cos(\theta_i^0-\theta_j^0) \ . \tag{1.3}$$

In (1.2) and (1.3), S is the spin, henceforth taken to be unity, θ_i^0 denotes the polar angle characterizing the spin orientation in the corresponding classical planar equilibrium configuration obtained by minimizing the "potential energy"

$$-\sum_{(i,j)} J_{ij}\cos(\theta_i-\theta_j) \ ,$$

and the ϕ_i denote the angles associated with the planar projections of the deviations of the spins from their equilibrium orientations. Spin-glass behavior was ensured by taking the exchange interactions, limited to nearest neighbors, to be a random variable having zero mean and unit variance.

The work reported in Ref. 6 was confined to $8\times8\times8$ simple-cubic arrays (512 spins) with periodic boundary conditions. Despite the limited size of the samples there was clear evidence for propagating modes with the dispersion relation $[I=S=\mathrm{Var}(J_{ij})=1]$:

$$\omega_k=0.52k \quad (\text{planar, 3D}) \ , \tag{1.4}$$

for a lattice constant equal to unity. In addition, the damping of the modes, as measured by the full width at half maximum of the peak in the dynamic structure factor, was found to be

$$\Gamma_k=0.24k^2 \quad (\text{planar, 3D}) \ . \tag{1.5}$$

The analysis begun in Ref. 6 was extended to two-dimensional arrays in Ref. 7. Just as in three dimensions, propagating modes were found in 24×24 square arrays (576 spins). They had the dispersion relation

$$\omega_k=0.50k \quad (\text{planar, 2D}) \ , \tag{1.6}$$

and full width at half maximum

$$\Gamma_k = 0.5k^2 \quad \text{(planar, 2D)} . \tag{1.7}$$

The results reported in Ref. 6 for the three-dimensional arrays were called into question in an investigation of the density of states which appeared to give evidence of a vanishing magnon velocity, and hence no propagating modes.[11] It is now believed that this interpretation is incorrect due to the insensitivity of the numerical method to small eigenvalues.[8,9]

Recently Grzonka and Moore[8] investigated the linearized magnon modes associated with the dynamical matrix (1.3) in arrays containing up to $22^3 = 10\,648$ spins in 3D and $64^2 = 4096$ spins in 2D. They calculated the limiting behavior of the density of states and found results consistent with a finite spin-wave velocity in both two and three dimensions. In addition, they made a direct calculation of the stiffness (square of the magnon velocity) by a spin-rotation method. In 3D their results showed a dependence on sample size which, when extrapolated to the infinite system limit, yielded a result equivalent to

$$\omega_k = 0.55k \quad \text{(planar, 3D)} . \tag{1.8}$$

In 2D they obtained results corresponding to the dispersion relation

$$\omega_k = 0.56k \quad \text{(planar, 2D)} . \tag{1.9}$$

In addition to calculating the stiffness Grzonka and Moore compared the limiting density of states calculated by direct diagonalization of the dynamical matrix with the density of states obtained assuming eigenmodes with the dispersion relations (1.8) and (1.9). From the analysis they concluded that the propagating modes contributed 80% of the density of states in two dimensions and only 40% in three dimensions. However, they were unable to identify the anomalous modes which gave rise to the enhanced density of states.

The magnon dispersion relations given by Eqs. (1.4) and (1.6) were inferred from a direct calculation of the dynamic structure factor which utilized the eigenvectors and eigenvalues obtained by diagonalizing the dynamical matrix.[6] Such a method is impractical for arrays as large as the ones studied in Ref. 8. However, the spin-rotation method which was employed might yield misleading results in the sense that the modes could have a finite stiffness and yet be overdamped. Such a situation appears to occur in Heisenberg spin glasses where similar calculations for the stiffness give nonzero values,[12,13] yet, as noted, there is no evidence of propagating modes in the dynamic structure factor.[4] For this reason it is important to calculate the dynamic structure factor directly. This we have done for arrays of $15\times15\times15 = 3375$ spins in three dimensions and $30\times30 = 900$ spins in two dimensions using equation-of-motion techniques developed by Alben and Thorpe.[14,15]

In addition to investigating the magnons associated with the planar Hamiltonian (1.1), we have also studied the linearized modes in the XY spin glass with the Hamiltonian

$$\mathscr{H} = -\sum_{(i,j)} J_{ij}(S_i^x S_j^x + S_i^y S_j^y) , \tag{1.10}$$

which generates the dynamical equations[6]

$$A_{ii}^{-1}\frac{d^2\phi_i}{dt^2} = -\sum_j A_{ij}\phi_j , \tag{1.11}$$

with A_{ij} given by Eq. (1.3). In subsequent sections of this paper we will discuss the application of equation-of-motion methods to the planar and XY models.

II. EQUATION-OF-MOTION METHODS

In applying equation-of-motion methods to the planar and XY spin glasses we will find it convenient to circumvent the second-order differential equations (1.2) and (1.11) and study instead the first-order equations

$$i\frac{du_i}{dt} = I^{-1}\sum_j A_{ij}u_j \tag{2.1}$$

and

$$i\frac{du_i}{dt} = A_{ii}\sum_j A_{ij}u_j . \tag{2.2}$$

Since both the second- and first-order problems are characterized by the same dynamical matrix, information about the properties of the modes can be obtained equally well from (2.1) and (2.2).

The Alben-Thorpe methods were originally developed for disordered ferromagnets and antiferromagnets.[14,15] We can make contact with their work by noting that equations formally equivalent to (2.1) can be generated for a ferromagnetic system with the magnon Hamiltonian

$$\mathscr{H} = I^{-1}\sum_{i,j}\alpha_i^\dagger A_{ij}\alpha_j , \tag{2.3}$$

where α_i and $\alpha_i^\dagger$ are the magnon annihilation and creation operators in the site representation. In transcribing the equations of Refs. 14 and 15 to planar spin glasses we make the following identification:

$$S\sum_k J_{ik} \to I^{-1}A_{ii} , \tag{2.4a}$$

$$-SJ_{ij} \to I^{-1}A_{ij} . \tag{2.4b}$$

In the case of the XY model one makes the replacement $u_i/A_{ii}^{1/2} \to v_i$ obtaining the symmetrized equations of motion

$$i\frac{dv_i}{dt} = \sum_j (A_{ii}A_{jj})^{1/2}A_{ij}v_j , \tag{2.5}$$

with a corresponding identification in terms of exchange integrals.

The equations of motion for the Green function $G_{ik}(t)$ which are integrated in calculating the dynamic structure factor take the form

$$i\frac{d}{dt}G_{ik}(t) = \sum_j \widetilde{A}_{ij}G_{jk}(t) , \tag{2.6}$$

with initial conditions $G_{ik}(0) = \delta_{ik}$. The matrix $\widetilde{A}_{ij}$ is given by

$$\widetilde{A}_{ij} = I^{-1}A_{ij} \tag{2.7}$$

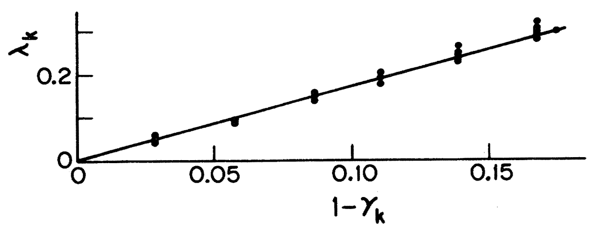

FIG. 1. λ_k vs $1-\gamma_k$ for the 3D planar model. The data are from five arrays of 15^3 spins. The solid line, $\lambda_k=1.71(1-\gamma_k)$, is a least-squares fit. The data in this and the other figures have calculated for models where I (planar model)$=S=$lattice constant$=\mathrm{Var}(J_{ij})=1$.

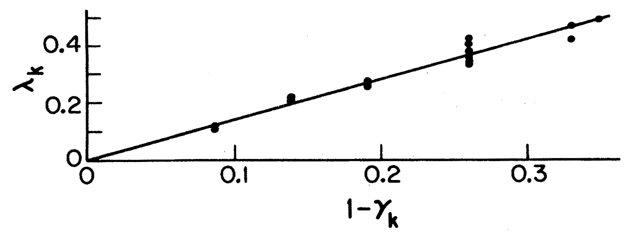

FIG. 3. λ_k vs $1-\gamma_k$ for the 2D planar model. The data are from three arrays of 30^2 spins. The solid line, $\lambda_k=1.40(1-\gamma_k)$, is a least-squares fit.

for the planar model (1.1), and by

$$\tilde{A}_{ij}=(A_{ii}A_{jj})^{1/2}A_{ij} \tag{2.8}$$

for the XY spin glass (1.10). Since from this point on the calculation of the dynamic structure factor parallels that of the disordered ferromagnet, we will not discuss the numerical analysis in any detail,[16] presenting only final results in Sec. III.

III. DYNAMIC STRUCTURE FACTOR

In our study of the spin dynamics we focused on the small-k behavior of the dynamic structure factor, $S(k,\lambda)$, calculated from the equivalent ferromagnetic magnon Hamiltonian

$$\mathscr{H}_{\mathrm{equiv}}=\sum_{i,j}\alpha_i^\dagger\tilde{A}_{ij}\alpha_j \;, \tag{3.1}$$

where $\tilde{A}_{ij}$ is given by (2.7) or (2.8). Since the analysis involves the integration of a set of coupled first-order differential equations whereas the underlying equations of motion, (1.2) and (1.11), are second order, the parameter λ is identified with the square of the frequency. In all cases studied $S(k,\lambda)$ was dominated by a single peak whose position we denote by λ_k.

In Fig. 1 we display our results for λ_k for the 3D planar spin glass. As in Ref. 6 we plot the data against $1-\gamma_k$, where γ_k is equal to

$$(\tfrac{1}{3})[\cos(k_x)+\cos(k_y)+\cos(k_z)] \;.$$

The solid line, $\lambda_k=1.71(1-\gamma_k)$, is a least-squares fit corresponding to the dispersion relation

$$\omega_k=\lambda_k^{1/2}\rightarrow 0.53k \quad (\text{planar, 3D}) \;, \tag{3.2}$$

in the limit as $k\rightarrow 0$.

In Fig. 2 we show corresponding results for the 3D XY spin glass. The least-squares fit is $\lambda_k=4.74(1-\gamma_k)$ leading to the limiting dispersion relation

$$\omega_k=0.89k \quad (XY,\ 3\text{D}) \;. \tag{3.3}$$

In Figs. 3 and 4 we display the results for the 2D systems. In both cases the data are plotted against $1-\gamma_k$, where now

$$\gamma_k=\tfrac{1}{2}[\cos(k_x)+\cos(k_y)] \;.$$

Figure 3 shows the data for the planar model. The solid line, $\lambda_k=1.40(1-\gamma_k)$, yields the limiting dispersion relation

$$\omega_k=0.59k \quad (\text{planar, 2D}) \;. \tag{3.4}$$

It should be noted that both (3.2) and (3.4) are in reasonable agreement with the estimates for the small arrays reported in Refs. 6 and 7 [cf. Eqs. (1.4) and (1.6)]. In Fig. 4 we present our results for the 2D XY spin glass. The solid line is $\lambda_k=2.31(1-\gamma_k)$ which corresponds to

$$\omega_k=0.76k \quad (\text{planar},\ XY) \;, \tag{3.5}$$

in the limit as $k\rightarrow 0$.

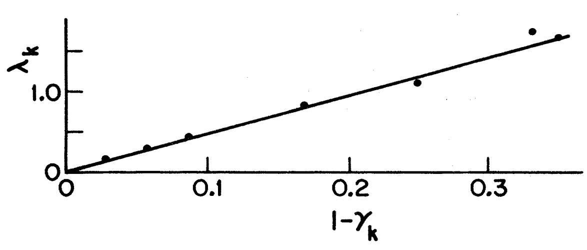

FIG. 2. λ_k vs $1-\gamma_k$ for the 3D XY model. The data are from a single array of 15^3 spins. The solid line, $\lambda_k=4.74(1-\gamma_k)$, is a least-squares fit.

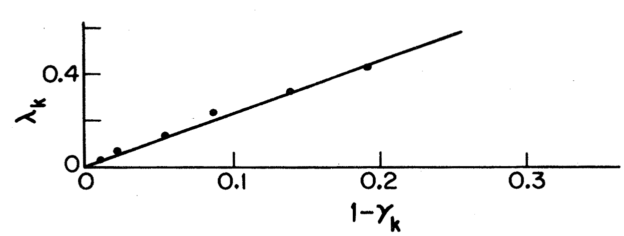

FIG. 4. λ_k vs $1-\gamma_k$ for the 2D XY model. The data are from a single array of 30^2 spins. The solid line, $\lambda_k=2.31(1-\gamma_k)$, is a least-squares fit.

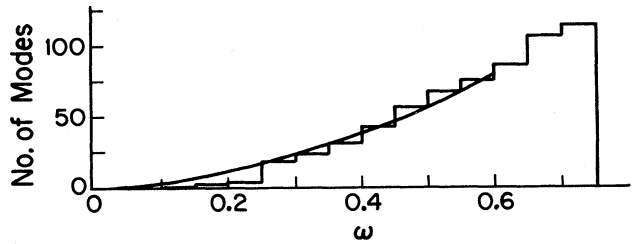

FIG. 5. Histogram for the distribution of eigenvalues, $\omega_k=\lambda_k{}^{1/2}$, for the 3D planar model. The data are from three arrays of 15^3 spins and the bin size is 0.05. The solid line is a quadratic fit corresponding to $\rho(\omega)=0.662\omega^2$.

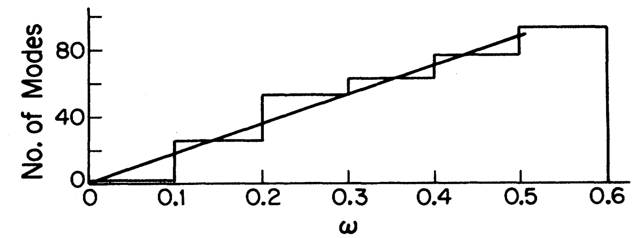

FIG. 7. Histogram for the distribution of eigenvalues, $\omega_k=\lambda_k{}^{1/2}$, for the 2D planar model. The data are from three arrays of 30^2 spins and the bin size is 0.1. The solid line is a linear fit corresponding to $\rho(\omega)=0.655\omega$.

IV. DENSITY OF STATES

In addition to the dynamic structure factor we have undertaken a calculation of the distribution of magnon modes using the negative eigenvalue theorem.[17,18] The normalized density of states $\rho(\omega)$ was fit to the functional form (D=dimension)

$$\rho(\omega)=\frac{\omega^{D-1}}{2\pi^{D-1}v^D}\,, \tag{4.1}$$

which is obtained assuming only propagating eigenmodes with the dispersion relation $\omega=vk$. Our results for the planar and XY models in 3D and 2D are shown in Figs. 5–8, along with the fits obtained using (4.1).[16] From the coefficient of ω^{D-1} we obtain the following effective velocities: $v_{\rm eff}$(planar, 3D)=0.42, $v_{\rm eff}$(XY, 3D)=0.56, $v_{\rm eff}$(planar, 2D)=0.49, $v_{\rm eff}$(XY, 2D)=0.64. These values are to be compared with the values obtained from the dynamic structure factor in Sec. III: v (planar, 3D)=0.53, v (XY, 3D)=0.89, v (planar, 2D)=0.59, and v (XY, 2D)=0.76. Since $v_{\rm eff}<v$, we find, in agreement with Ref. 8, that the densities of states are enhanced relative to the results obtained using (4.1) with magnon velocities inferred from either the stiffness or the dynamic structure factor. We return to this point in the next section.

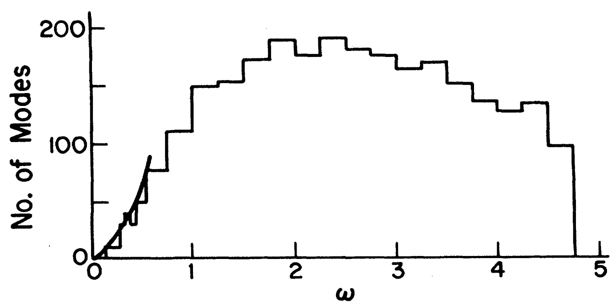

FIG. 6. Histogram for the distribution of eigenvalues, $\omega_k=\lambda_k{}^{1/2}$, for the 3D XY model. The data are from a single array of 15^3 spins and the bin size is 0.25. The solid line is a quadratic fit corresponding to $\rho(\omega)=0.296\omega^2$.

V. DISCUSSION

Prior to taking up the question of the enhanced density of states we compare our magnon velocities and densities of states for the planar model with those reported in Ref. 8. In that reference the stiffness parameter, or magnon velocity squared, was found to depend on sample size in 3D varying according to

$$v^2=0.308+\frac{75.728}{N}\quad\text{(planar, 3D)}\,, \tag{5.1}$$

where N is the number of spins. For $N=15^3$ one obtains v=0.57 which is approximately 8% larger than 0.53, the value inferred from the dynamic structure factor. It should be noted that the latter value (0.53) is close to 0.55, the $N=\infty$ limit of (5.1). In two dimensions the magnon velocities reported in Ref. 8 were independent of sample size ($1024<N<4096$) with an average value equal to 0.56, which is approximately 5% less than 0.59, the value inferred from the dynamic structure factor of the 2D planar model.

For the density of states Grzonka and Moore[8] report the following: $\rho(\omega)=(0.666\pm0.012)\omega^2$ for the 3D planar model (N=4096) and $\rho(\omega)=(0.660\pm0.014)\omega$ for the planar model in two dimensions (N=1600). Our results take the form $\rho(\omega)=0.662\omega^2$ (N=3375) and $\rho(\omega)=0.655\omega$ (N=900) for the equivalent models. From these comparisons we conclude (1) that both the stiffness calculation and the equation-of-motion methods give comparable results for the magnon velocity, and (2) the spin-relaxation procedures used to obtain the equilibrium configurations

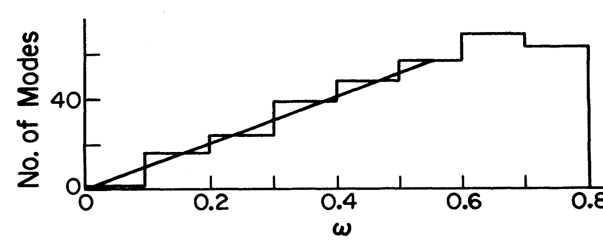

FIG. 8. Histogram for the distribution of eigenvalues, $\omega_k=\lambda_k^{1/2}$, for the 2D XY model. The data are from three arrays of 30^2 spins and the bin size is 0.1. The solid line is a linear fit corresponding to $\rho(\omega)=0.383\omega$.

in our work and in that of Ref. 8 lead to virtually identical excitation spectra.

The results reported in this paper, along with those of Refs. 6–9, support the prediction of weakly damped, propagating modes in easy plane spin glasses.[19] The observation of the modes in both the planar model [Eq. (1.2)] and the XY model [Eq. (1.11)] suggests they are a universal feature of such systems. As noted, the magnon velocities inferred from the dynamic structure factor for the planar model differ from the values obtained from a numerical calculation of the stiffness by less than 10%. Because of this agreement our results do not shed any direct light on the enhancement of the density of states. It was suggested in Ref. 8 that this enhancement could reflect the presence of low-lying, nonpropagating modes. Although we cannot rule out this explanation, the fact that these modes must have a density of states with the same functional dependence on frequency as that of the propagating modes is difficult to understand. It is possible that the discrepancy arises because the propagating modes have a non-negligible width at finite k [cf. Eqs. (1.5) and (1.7)] and hence are only approximate eigenvectors of the dynamical matrix. As a consequence they may not give a quantitatively accurate representation of the eigenvalue spectrum. The fact that the exact density of states and the density of states obtained from (4.1) have the same frequency dependence would indicate a one-to-one correspondence between the low-lying eigenstates and the propagating modes with the corresponding frequencies being related by a scale factor (which is perhaps equally difficult to understand).

ACKNOWLEDGMENTS

We would like to thank R. B. Grzonka and M. A. Moore for providing us with a copy of the report on their work prior to publication. The research was supported by the National Science Foundation under Grant No. DMR-82-03704.

*Present address: Sperry Corporation, Egan, MN 55121.

1A. J. Bray and M. A. Moore, J. Phys. C **14**, 2629 (1981).
2D. L. Huber and W. W. Ching, *Amorphous Magnetism II*, edited by R. A. Levy and R. Hasegawa (Plenum, New York, 1977), p. 39.
3B. I. Halperin and W. M. Saslow, Phys. Rev. B **16**, 2154 (1977).
4W. Y. Ching, D. L. Huber, and K. M. Leung, Phys. Rev. B **23**, 6126 (1981).
5W. Y. Ching and D. L. Huber, Phys. Rev. B **27**, 5810 (1983).
6D. L. Huber, W. Y. Ching, and M. Fibich, J. Phys. C **12**, 3535 (1979).
7D. L. Huber and W. Y. Ching, J. Phys. C **13**, 5579 (1980).
8R. B. Grzonka and M. A. Moore, J. Phys. C **16**, 1109 (1983).
9A. J. Bray, R. B. Grzonka, and M. A. Moore, J. Magn. Magn. Mater. **31-34**, 1293 (1983).
10J. Villain, J. Phys. (Paris) **35**, 27 (1974).
11A. J. Bray and M. A. Moore, Phys. Rev. Lett. **47**, 120 (1981).
12P. Reed, J. Phys. C **12**, L475 (1979).
13R. E. Walstedt, Phys. Rev. B **24**, 1524 (1981).
14R. Alben and M. F. Thorpe, J. Phys. C **8**, L275 (1975).
15M. F. Thorpe and R. Alben, J. Phys. C **9**, 2555 (1976).
16For the details of the calculations see C. M. Grassl, Ph.D. thesis, University of Wisconsin—Madison, 1983.
17P. Dean, Proc. R. Soc. London **A254**, 507 (1960); **A260**, 263 (1961).
18P. Dean and J. L. Martin, Proc. R. Soc. London **A259**, 409 (1960).
19S. F. Edwards and P. W. Anderson, J. Phys. F **6**, 1927 (1976).